

## Studies on Preparation and Characterization of 45S5 Bioactive Glass Doped with ( $\text{TiO}_2 + \text{ZrO}_2$ ) as Bioactive Ceramic Material

Himanshu T\*, Singh SP\*, Sampath KA, Prerna M and Ashish J

Department of Ceramic Engineering, Indian Institute of Technology, Banaras Hindu University, Varanasi, India

### Abstract

The aim of the present investigation was to evaluate the role of  $\text{TiO}_2 + \text{ZrO}_2$  in the system of 45S5 bioactive glass for improving the bioactivity as well as other physical and mechanical properties of 45S5 bioactive glass. The partial substitution of 1, 2, 3 and 4 mol% of mixed  $\text{TiO}_2 + \text{ZrO}_2$  (3:2) for  $\text{SiO}_2$  in 45S5 bioactive glass system was done by melting route at  $1400^\circ\text{C}$  in a global rod furnace in air. A comparative study on structural and mechanical properties, as well as bioactivity of the glasses, was reported. The glass properties were determined by XRD, FTIR spectrometry, SEM and the bioactivity of the glass samples were evaluated by *in vitro* test in simulated body fluid (SBF). Density and compressive strength of glass samples were measured. Results indicate that with the partial substitution of  $\text{TiO}_2 + \text{ZrO}_2$  for  $\text{SiO}_2$  in 45S5 bioactive glass system, the mechanical properties of the glasses were found to increase significantly. The glass samples exhibited higher density and compressive strength as compared to their corresponding 45S5 bioactive glass. The *in vitro* studies of glass samples in SBF had shown that the pH of the solution increased with increasing the time period for immersion during the initial stage of the reaction. This indicated the bioactivity of the samples had increased with increasing duration. On later stages, the decrease in pH of the solution with time had shown that the bioactivity of the samples had decreased.

**Keywords:** Bioactive glass; Simulated body fluid; FTIR spectrometry; Ceramics; Phosphate-based glasses; Borate-based glasses

### Introduction

Bioactive glasses have been widely investigated for bone repair because of their outstanding bioactive properties. However, these bioactive materials undergo incomplete conversion into a bone-like material which severely limits their biomedical application [1]. When bioactive glasses are soaked in simulated body fluid, they bind to living bone through an appetite layer formed on their surfaces. The mechanism of the reaction for bonding the implant to the bone was given by Clark and Hench [2]. One of the main characteristics of the bioactive glasses is their highly reactive surface. Hench decided to make a glass in the  $\text{SiO}_2\text{-Na}_2\text{O-CaO-P}_2\text{O}_5$  system, high in calcium content and with a composition close to a ternary eutectic in the  $\text{Na}_2\text{O-CaO-SiO}_2$  diagram [3]. The main discovery was that a glass of the mol% composition 46.1  $\text{SiO}_2$ , 24.4  $\text{Na}_2\text{O}$ , 26.9  $\text{CaO}$  and 2.6  $\text{P}_2\text{O}_5$ , later termed 45S5 and Bioglass, formed a bond with the bone so strong that it could not be removed without breaking the bone [4]. This launched the field of bioactive ceramics, with many new materials and products being formed from variations on bioactive glasses, glass-ceramics [5] and ceramics such as synthetic hydroxyapatite (HA) and other calcium phosphates [6]. Herein, a bioactive material is defined as a material that stimulates a beneficial response from the body, particularly bonding to host tissue (usually bone). The term “bioceramic” is a general term used to cover glasses, glass-ceramics and ceramics that are used as implant materials. Bioglass 45S5 is widely used in biomedical devices, such as middle ear and dental implants. However, its relatively low strength and brittleness limit its application to non-load bearing situations [7]. There are now several types of bioactive glasses: the conventional silicates, such as Bioglass 45S5; phosphate-based glasses; and borate-based glasses. Recently, interest has increased in borate glasses [8] largely due to very encouraging clinical results of healing the chronic wounds, such as diabetic and ulcers, which would not heal under conventional treatment [9]. The soft tissue response may be due to their fast dissolution, which is more rapid than that for silica-based glasses. The benefits of phosphate glasses are also likely to be related to their very rapid solubility rather than bioactivity [10]. In order to

improve the mechanical reliability of glass-based biomedical devices, various approaches have been proposed, such as the production of sintered bodies or the deposition of coatings. However, the BG-45S5, like other bioactive glasses, tends to crystallize at high temperature, due to its relatively low content of silica [11]. This is a relevant drawback since the crystallization is thought to reduce the bioactivity of the glass [12,13] and on the other hand, thermal treatments are widely required to obtain not only special products, such as sintered glass scaffolds or glass fibers but also ordinary coatings [11]. The addition of elements like magnesium, aluminum, zirconia, or titanium may be used to control some physical and chemical properties of bioglasses [14,15]. When the bioglass is doped with  $\text{TiO}_2$ , the apatite can be formed biomimetically on the surface of bioglass immersed in simulated body fluid. Titania has a tendency to adsorb water at the surface, resulting in the formation of titanium hydroxide groups. The basic Ti-OH groups were reported to induce apatite nucleation and crystallization in simulated body fluid [16]. The production of composite materials has proved to be the suitable solutions for improving the mechanical properties of weaker materials. Ceramic biocomposites were reinforced by introducing another tough phase of  $\text{Al}_2\text{O}_3$  and  $\text{ZrO}_2$  [15]. The yttria-stabilized zirconia was introduced into orthopedic surgery in the late eighties as a new generation ceramic material [17]. Zirconia is particularly attractive as a reinforcing phase since it is bio-inert and HA/ $\text{ZrO}_2$  composites give significantly improved mechanical properties [18]. Therefore, in

**\*Corresponding authors:** Himanshu T and Singh SP, Department of Ceramic Engineering, Indian Institute of Technology, Banaras Hindu University, Varanasi, India, Tel: 0542 236 8106; E-mail: [himanshutripath@gmail.com](mailto:himanshutripath@gmail.com), [spsinghceram@gmail.com](mailto:spsinghceram@gmail.com)

**Received** December 18, 2015; **Accepted** January 28, 2016; **Published** February 08, 2016

**Citation:** Himanshu T, Singh SP, Sampath KA, Prerna M, Ashish J (2016) Studies on Preparation and Characterization of 45S5 Bioactive Glass Doped with ( $\text{TiO}_2 + \text{ZrO}_2$ ) as Bioactive Ceramic Material. Bioceram Dev Appl 6: 090. doi:10.4172/2090-5025.100090

**Copyright:** © 2016 Himanshu T, et al. This is an open-access article distributed under the terms of the Creative Commons Attribution License, which permits unrestricted use, distribution, and reproduction in any medium, provided the original author and source are credited.

the present investigation; the 45S5 bioactive glass has been taken as a reference. The concentration of SiO<sub>2</sub> was varied by mol% addition of TiO<sub>2</sub>+ZrO<sub>2</sub> in the ratio of (3:2) from 1-4 mol%, respectively in the 45S5 bioactive glass. The purpose of this work is to provide information on bioactivity assessment and to increase the other physical and mechanical properties of 45S5 bioactive glass by introducing 1-4 mol% TiO<sub>2</sub>+ZrO<sub>2</sub> into it.

## Materials and Methods

### Sample preparation

The mol% compositions of the bioglass samples are shown in Table 1. Fine-grained quartz was used for silica (SiO<sub>2</sub>). Analytical reagent grade CaCO<sub>3</sub>, Na<sub>2</sub>CO<sub>3</sub> and ammonium dihydrogen orthophosphate (NH<sub>4</sub>H<sub>2</sub>PO<sub>4</sub>) (Merck specialities private limited, Mumbai, India, Assay 99.8%) were used as a source of CaO, Na<sub>2</sub>O and P<sub>2</sub>O<sub>5</sub>, respectively. The required amounts of analytical reagent grade (Merck specialities private limited, Mumbai, India, and Assay 99.8%) TiO<sub>2</sub> and ZrO<sub>2</sub> were added in the batch for the partial substitution of silica. The proper raw materials for different samples were weighted. Then the mixing of different batches was done for 30 minutes and melted in alumina crucibles. The thermal cycle was set for all glass samples: from room temperature to 1000°C at 10°C/min; at 1000°C for 1 hour; from 1000°C to 1400°C at 10°C/min; at 1400°C for 2 hours. The melting of samples was done in the electronic globar furnace, air as the furnace atmosphere. The melted samples were poured on a preheated aluminum sheet and directly transferred to a regulated muffle furnace at 450°C for annealing and after 1 hour of annealing of the samples, muffle furnace was cooled to the room temperature at the rate of 1.5°C/min. The half parts of the samples were crushed in a pestle mortar and then ground in an agate mortar to make fine powders of the samples for different properties measurements by different experimental techniques. The other half of solid glass samples were used for density and compressive strength measurements.

### In-vitro analysis of bioactive glass samples

The *in vitro* bioactivity assessments of the glasses were carried out by their immersion in simulated body fluid (SBF) solutions for 1 to 28 days at 37.4°C. The simulated body fluid (SBF) solutions were prepared according to the formula described by Kokubo[19]. Table 2 shows the ion concentrations of the SBF solution. The glass samples in the form of pellet having the size of 1 cm diameter were immersed in SBF at 37.4°C for different time periods varying from 1 to 28 days. The pH of the SBF solutions was measured using digital pH meter for different time periods.

### Structural analysis of bioglasses by FTIR transmittance spectroscopy

The *in-vitro* bioactivity of chemically treated samples in SBF solution was assessed by evaluating the formation of carbonated hydroxy calcium phosphate layer on the surface of the samples before and after immersion in SBF solution using FTIR transmittance spectroscopy. The infrared transmittance spectra of the bioglasses were recorded at the room temperature in the spectral range 4000-400 cm<sup>-1</sup> using a Fourier Transform Infra-Red spectrometer (Shimadzu-8400S, Japan).

### Microstructure analysis using scanning electron microscope

The surfaces of bioactive glasses were analyzed before and after immersion in SBF. The samples were coated with plasma gold plate

before measurement with SEM. A scanning electron microscope (Inspect 50 FEI) was used to find the surface microstructure of bioactive glass samples.

### Density and compressive strength measurements

The densities of the samples were determined by Archimedes' principle with water as the immersion liquid. The measurements were carried out at room temperature. The compressive strength of bioactive glass samples was measured by a universal testing machine. The solid glass samples were in cubical shape (1 cm × 1 cm × 1 cm). Further, the samples were subjected to compression load and the test was performed using Universal Testing Machine (Shimadzu, Japan) at room temperature (cross speed of 5 mm/min). Five glass samples of each group were used for each data point. The compressive strength was calculated using the following equation:

$$\text{Compressive strength: } (\sigma_c) = \frac{F}{A}$$

Where F is the maximum compressive load during the test (N), A is the initial area of the specimen (cm<sup>2</sup>).

## Results and Discussion

### Density and compressive strength of bioactive glass samples

The results in Table 3 show the density and Figure 1 shows the compressive strength of bioactive glass samples in the form of error bars. It is observed that the densities of the samples were found to increase with increasing TiO<sub>2</sub>+ZrO<sub>2</sub> content in the glass from 2.54 to 2.89 gm/cc with the increasing amount of TiO<sub>2</sub>+ZrO<sub>2</sub> contents into the bioactive glass samples. From the Figure 1 it is also clear that with the increasing amount of TiO<sub>2</sub>+ ZrO<sub>2</sub> the compressive strength of samples has increased from 54 to 65 MPa. It may be due to partial replacement of SiO<sub>2</sub> with TiO<sub>2</sub>+ZrO<sub>2</sub> which is attributed due to the replacement of

	SAMPLE	SiO <sub>2</sub>	Na <sub>2</sub> O	CaO	P <sub>2</sub> O <sub>5</sub>	TiO <sub>2</sub> +ZrO <sub>2</sub> (3:2)
1	45S5	46.1	24.4	26.9	2.6	0
2	TZ1	45.1	24.4	26.9	2.6	1
3	TZ2	44.1	24.4	26.9	2.6	2
4	TZ3	43.1	24.4	26.9	2.6	3
5	TZ4	42.1	24.4	26.9	2.6	4

**Table 1:** Mol% composition of bioactive glass samples.

	Ion	Concentration (mM)
1	Na <sup>+</sup>	142.0
2	K <sup>+</sup>	5.0
3	Mg <sup>2+</sup>	1.5
4	Ca <sup>2+</sup>	2.5
5	Cl <sup>-</sup>	147.8
6	HCO <sub>3</sub> <sup>-</sup>	4.2
7	HPO <sub>4</sub> <sup>2-</sup>	1.0
8.	SO <sub>4</sub> <sup>2-</sup>	0.5

**Table 2:** The ions concentration of the SBF solution (mM).

Serial No	Sample Name	Density (gm/cc)
1	45S5	2.54
2	TZ1	2.70
3	TZ2	2.76
4	TZ3	2.80
5	TZ4	2.89

**Table 3:** Density of bioactive glass samples (gm/cc).

a smaller ion (Si<sup>4+</sup>) with a bigger Ti<sup>4+</sup> and Zr<sup>4+</sup> ions in the glass. In other words, the lighter molar mass of SiO<sub>2</sub> (60.08 g/mol) has been replaced by the heavier TiO<sub>2</sub> (79.86 gm/mol) and ZrO<sub>2</sub> (123.22 gm/mol) in the bioactive glass samples.

### X-Ray diffraction analysis of bioactive glass samples

X-ray diffraction patterns were observed using a Rigaku portable XRD machine (Rigaku, Tokyo, Japan). Phase identification analysis was carried out by comparing the XRD patterns of the bioactive glass samples to the standard database stated by JCPDS which is indicated in Figure 2a and it shows the XRD plots of the bioactive glass samples before soaking them into the simulated body fluid (SBF). Before being soaked in SBF solutions, there was no XRD absorption peak for the bioactive glass samples, except for one bump like peak ranging from 20° to 30°, which is due to Si-O-Si network. So it is clear that bioactive glass samples were amorphous in nature before being soaked in simulated body fluid (SBF) solution. While Figure 2b shows the XRD plots of the bioactive glass samples soaked in the simulated body fluid (SBF) solution for 14 days. After being soaked in the SBF solution for 14 days, one diffraction peak was observed at a 2θ angle of 31.9°, corresponding to the HA phase. These peaks were identified by standard JCPDS cards numbered 89-6495.

### In-vitro analysis of bioactive glass samples

Figure 3 shows the variation of pH of bioactive glass samples after immersing in simulated body fluid (SBF) solution for 1 to 28 days. Greenspan also confirmed that changes in pH of glass samples took place after immersion in simulated body fluid (SBF) solution [20]. It shows that for all bioactive glass samples, the pH increases within 1 to 7 days as compared to the initial pH of the SBF solution at 7.4. The increase in pH values is due to the fast release of Na<sup>+</sup> and Ca<sup>2+</sup> ions through exchange with H<sup>+</sup> or H<sub>3</sub>O<sup>+</sup> ions into the simulated body fluid (SBF) solution. The H<sup>+</sup> ions are being replaced by cations which cause an increase in hydroxyl concentration of the solution. This leads to attack in the silica glass network, which results in the formation of silanols leading to decrease in pH which is indicated in the Figure 3 as bioactive glass samples immersed in simulated body fluid (SBF) solution for 7 to 28 days. The change in pH was due to ion leaching. The increase in pH of SBF solution shows a decrease in the concentration of H<sup>+</sup> ions due to the replacement of cations in the bioactive glass. It was also seen that the decrease in the pH of the SBF solution after 15 days as a result of breaking of glass network. Morphological properties of bioactive glasses also indicate that soaking in SBF lead to the formation of an apatite layer [21,22] on the surface of the samples. There are five proposed stages for HA formation in body fluid in simulated body fluid (SBF) *in vitro* [1,23].

1. Rapid cation exchange of Na<sup>+</sup> and/or Ca<sup>2+</sup> with H<sup>+</sup> from solution, creating silanol bonds (Si-OH) on the glass surface: Si-O-Na<sup>+</sup> + H<sup>+</sup> + OH<sup>-</sup> → Si-OH + Na<sup>+</sup> (aq) + OH<sup>-</sup>
2. The pH of the solution increases and a silica-rich (cation-depleted) region forms near the glass surface. Phosphate is also lost from the glass if present in the composition.
3. High local pH leads to attack of the silica glass network by OH<sup>-</sup>, breaking Si-O-Si bonds. Soluble silica is lost in the form of Si(OH)<sub>4</sub> to the solution, leaving more Si-OH (silanols) at the glass-solution interface: Si-O-Si + H<sub>2</sub>O → Si-OH + OH-Si
4. Condensation of Si-OH groups near the glass surface: repolymerization of the silica-rich layer.

5. Migration of Ca<sup>2+</sup> and PO<sub>4</sub><sup>3-</sup> groups to the surface through the silica-rich layer and from the solution, forming a film rich in amorphous CaO-P<sub>2</sub>O<sub>5</sub> on the silica-rich layer.
6. Incorporation of hydroxyls and carbonate from solution and crystallization of the CaO-P<sub>2</sub>O<sub>5</sub> film to HA.

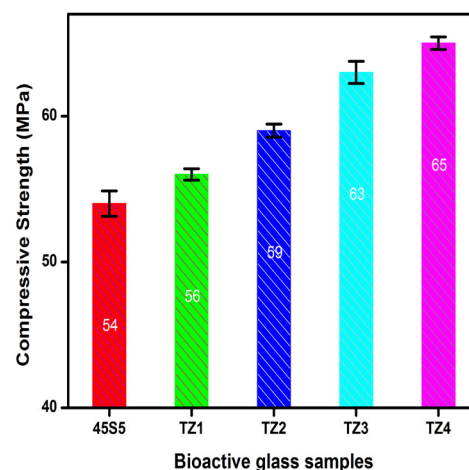


**Figure 1:** Variation of compressive strength with composition of the bioactive glass samples.

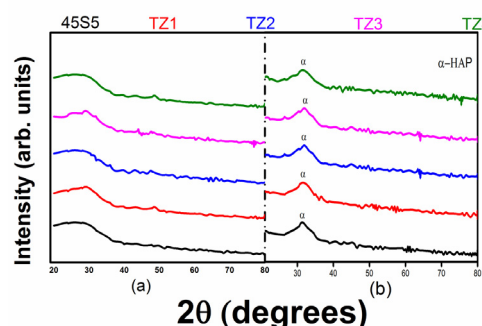


**Figure 2:** (a) XRD patterns of bioactive glass samples before immersing the samples in SBF. (b) XRD patterns of bioactive glass samples after immersing the samples in SBF for 14 days.

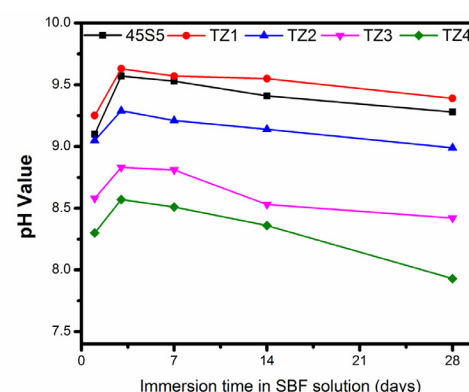


**Figure 3:** Variation of pH of the SBF solution containing glass samples with different time intervals.



## SEM analysis of bioactive glass samples

**SEM analysis of bioactive glass samples before soaking in SBF solution:** The SEM micrographs of bioactive glass samples before soaking in SBF solution are shown in Figure 4 which shows different rod type structures and irregular grains of bioactive glass samples which is quite similar to the result found by Hanan [24].

**SEM analysis of bioactive glass samples after soaking in SBF solution:** Figure 5 shows the SEM micrographs of bioactive glass samples after soaking in SBF solution for 14 days. It is clear from the Figure 5 that bioactive glass samples which were soaked in SBF solution for 14 days were covered with irregular shape and grounded HA particles have been grown into several agglomerates consisting of needle-shaped HA layer. These micrographs show the formation of HA on the surface of bioactive glass samples after immersion in SBF solution for 14 days.

## Transmission-FTIR analysis of bioactive glass samples before and after immersion in SBF solution

Figures 6-10 show the corresponding transmission FTIR analysis of bioactive glass samples before and after immersion in SBF solution for 1 to 14 days. The transmission spectra of all bioglass samples before soaking them in SBF solution exhibit vibrational bands at around 440 cm<sup>-1</sup> due to Si-O-Si bending [25]. The FTIR spectra of bioactive glass samples after soaking in simulated body fluid (SBF) solution for different times reveal Si-O-Si tetrahedral (840-720 cm<sup>-1</sup>) which indicates the formation of the silica-rich layer. The presence of P-O bonding (amorphous) (560-550 cm<sup>-1</sup>) bands indicates the formation of calcium phosphate (CaO-P<sub>2</sub>O<sub>5</sub>) layer [26]. In addition to these other bands were also found to be centered at around 1420 and 1480 cm<sup>-1</sup> which are attributed due to carbonate groups [CO<sub>3</sub>]<sup>2-</sup> indicating the precipitation of B-type hydroxy carbonate apatite, (Ca<sub>3</sub>(HPO<sub>4</sub>)<sub>0.5</sub>(CO<sub>3</sub>)<sub>0.5</sub>(PO<sub>4</sub>)<sub>3</sub>OH) (HCA) mimicking bone like apatite in the system [27]. The presence of carbonate groups [CO<sub>3</sub>]<sup>2-</sup> (1400-1500 cm<sup>-1</sup>) bands show the crystalline nature of HA layer and their bands are attributed due to HA layer [28,29]. The bands were observed at 1560 and above 3500 cm<sup>-1</sup> in the spectra which are attributed due to presence of OH group because of water adsorption in the system [30]. Intensity of silica-rich layer and CaO-P<sub>2</sub>O<sub>5</sub> layer goes on decreasing but the intensity of HA layer increases with time in all cases after soaking for 1 day in SBF solution. Hench was the first to detail a number of sequential steps in the *in vitro* and *in vivo* reactivity of silicate glasses that are responsible for the tissue bonding ability of these glasses. Briefly, these involve cation release from the glass with a consequential increase in pH of solution, formation of silica-rich layer and precipitation of a CaO-P<sub>2</sub>O<sub>5</sub> rich layer that further crystallizes as HA layer [1,31]. The degree of bioactivity is expressed by the formation of HA layer. Finally, the FTIR transmittance spectra of bioactive glasses after soaking for 14 days in SBF solutions, Figures 6-10 indicates that addition of more than 1 mol% of TiO<sub>2</sub>+ZrO<sub>2</sub> in the base bioactive glass (45S5) decreases its bioactivity. This is because of the fact that transition metals enhance the chemical durability of silicate glasses [32]. The precipitation of pure hydroxyapatite in SBF is likely to happen less because it is saturated with respect to slightly carbonated apatite, in which the orthophosphates are substituted with carbonates in the crystal lattice [33]. Gibson, et al. [34] pointed out that the P-O bending bands, at 546 cm<sup>-1</sup> in the FTIR spectra were not characteristic to HA or HCA, but they indicate the presence of orthophosphate lattices. Therefore, the phases formed at the surface of the bioactive glass samples were also confirmed by X-ray diffraction as shown in Figure 2. So our results regarding the formation of HCA

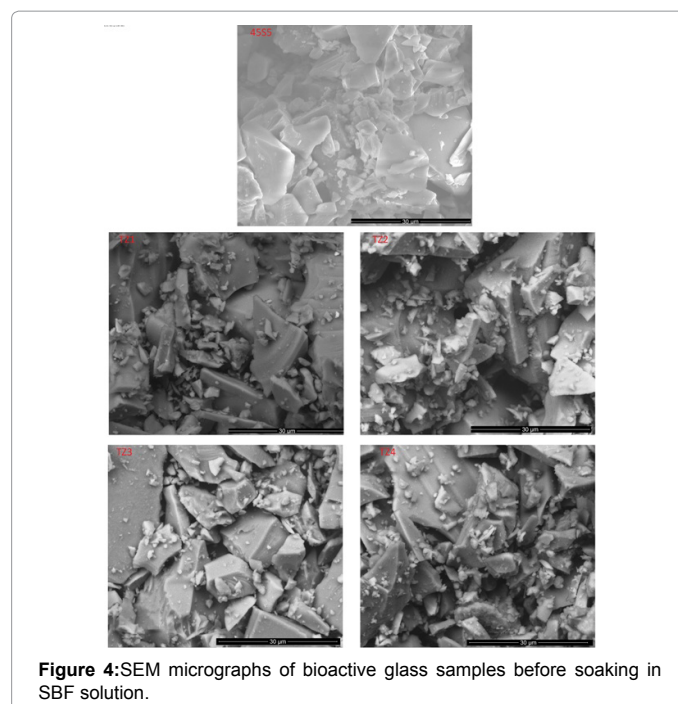


**Figure 4:** SEM micrographs of bioactive glass samples before soaking in SBF solution.

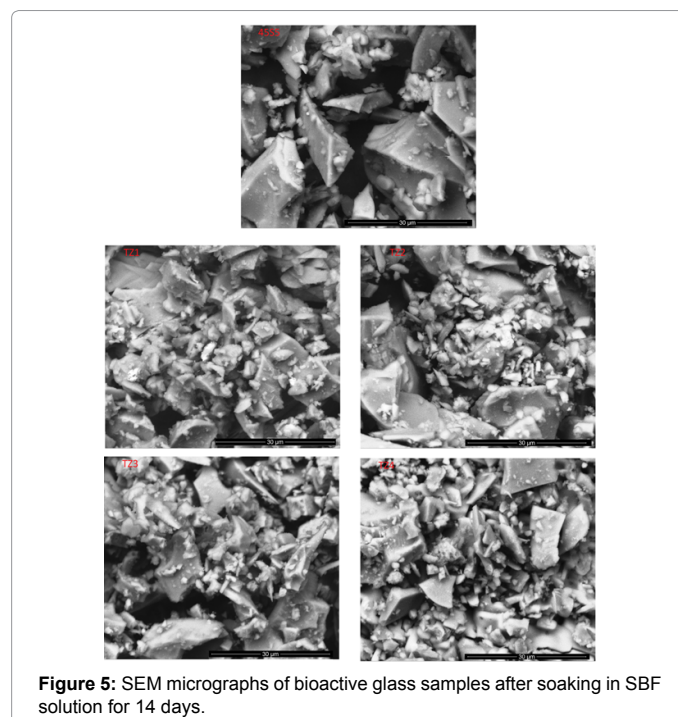


**Figure 5:** SEM micrographs of bioactive glass samples after soaking in SBF solution for 14 days.

in SBF by FTIR transmission spectrometry are well supported by the observations made by Anthony [27].

## Conclusions

In the present investigation, a comparative study was made on physical, bioactive and mechanical properties of TiO<sub>2</sub>+ZrO<sub>2</sub> substituted 45S5 bioactive glasses. The following conclusions are obtained from this investigation:

1. On increasing the substitution of TiO<sub>2</sub>+ZrO<sub>2</sub> for SiO<sub>2</sub> in the bioactive

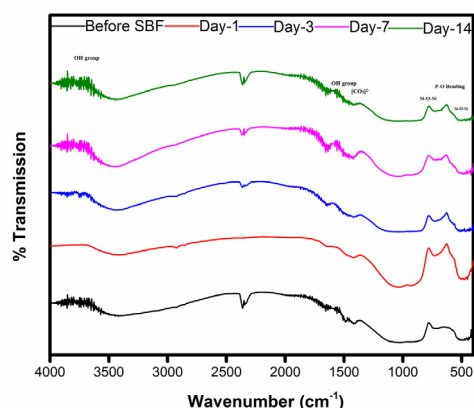


**Figure 6:** FTIR transmission spectra of 45S5 bioactive glass sample before and after SBF treatment.

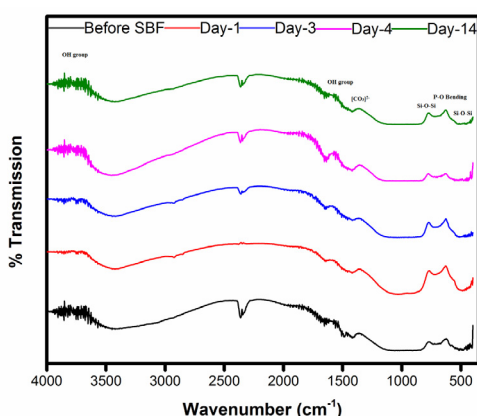


**Figure 7:** FTIR transmission spectra of bioactive glass sample TZ1 before and after SBF treatment.

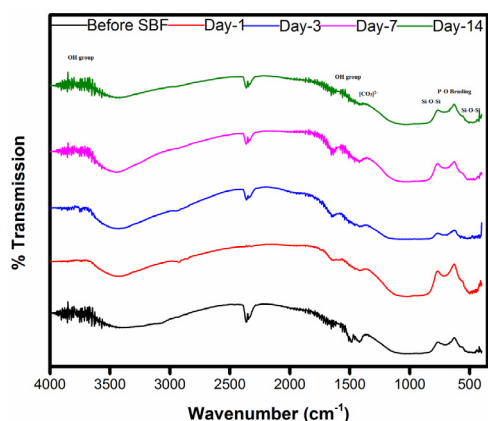


**Figure 8:** FTIR transmission spectra of bioactive glass sample TZ2 before and after SBF treatment.

glass 45S5, density and compressive strength were found to increase accordingly.

- The transmission FTIR spectra showed different characteristics bands because of silicate network which indicated the formation of the hydroxy calcium apatite (HA) layer on the surface of bioactive glass samples after immersing in SBF from 1 to 28 days.

- The bioactivity of these samples was measured by *in-vitro* analysis in SBF solution for 1 to 28 days. The pH of the solution was found to increase from 1 to 3 days and nearly constant up to 7 days. After 7 days the pH of the glass samples decreased that shows the samples were bioactive. An increase in the pH of the SBF shows the relative increase in bioactivity of the sample immersed in the solution. Because the increase in pH values of the solution is due to fast release of cations through exchange with H<sup>+</sup> or H<sub>3</sub>O<sup>+</sup> ions in the simulated body fluid (SBF) solution. The H<sup>+</sup> ions are being replaced by cations which cause an increase in hydroxyl ion (OH<sup>-</sup>) concentration of the solution due to formation of their hydroxides. This leads to attack on the silica glass network, which results in silanols (Si-OH) formation in the solution. Further condensation and polymerization of silanols occurs at glass surface which results in the formation of SiO<sub>2</sub>-rich layer. The migration of Ca<sup>2+</sup> and PO<sub>4</sub><sup>3-</sup> ions from the solution takes place on silica rich layer and form amorphous CaO-P<sub>2</sub>O<sub>5</sub> layer. The incorporation of carbonate ions (CO<sub>3</sub>)<sup>2-</sup> from the solution into amorphous CaO-P<sub>2</sub>O<sub>5</sub> layer results in the formation of crystalline hydroxy carbonate apatite layer (HCA) on the surface of the glass samples. Thus, the surface of the glass samples is covered by the bioactive HCA [Ca<sub>10</sub>(PO<sub>4</sub>)<sub>6-*x*</sub>(CO<sub>3</sub>)<sub>*x*</sub>(OH)<sub>2-*x*</sub>, where 0 ≤ *x* ≤ 2 interface. The formation of HCA layer on the surface of the glass sample causes the termination of the contact between the sample and the SBF solution. This leads to a decrease in pH of the solution after 3 days as indicated in the Figure 3 when

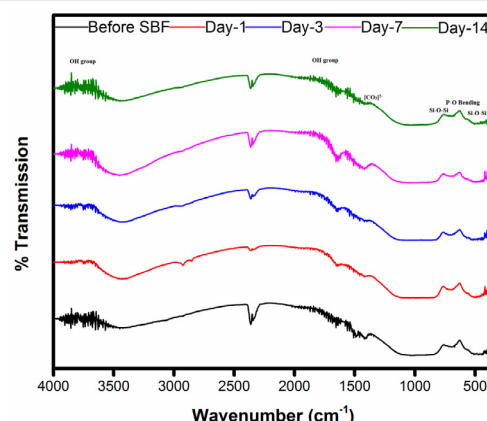


**Figure 9:** FTIR transmission spectra of bioactive glass sample TZ3 before and after SBF treatment.

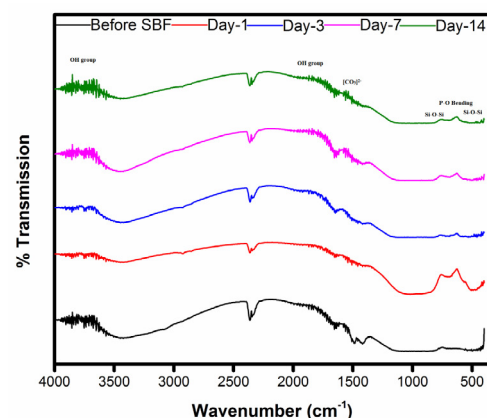


**Figure 10:** FTIR transmission spectra of bioactive glass sample TZ4 before and after SBF treatment.

bioactive glass samples were immersed in simulated body fluid (SBF) solution up to 28 days. The high degradation rate leads to higher pH value. Based on the above mechanism, an increase in the pH value of SBF solution also favors the hydroxy carbonate apatite formation leading to an increase in bioactivity of the samples. 4. The addition of TiO<sub>2</sub>+ZrO<sub>2</sub> beyond 1 mol% caused a decrease in maxima of the pH of the SBF solution containing immersed samples. This dictates that addition of TiO<sub>2</sub>+ZrO<sub>2</sub> up to 1 mol% in the glass samples has increased its bioactivity, but beyond 1 mol% of TiO<sub>2</sub>+ZrO<sub>2</sub> retards the bioactivity of the glass samples (Figure 3).

5. The SEM analysis of these samples before soaking in SBF shows the different irregular grains of glass samples. While after 14 days of SBF treatment, HA layer was formed on the surface of these samples due to its bioactive nature. Thus, we can say that substitution of TiO<sub>2</sub>+ZrO<sub>2</sub> for SiO<sub>2</sub> in the bioactive glass 45S5 would be good bioactive materials which have more mechanical properties with the comparison to bioactive glass 45S5.

### Acknowledgements

The authors gratefully acknowledge Mr. Ashih Tripathi, Mr. Bhagmal Singh, Mr. R.A.Yadav and other nonteaching staff of the Department of Ceramic Engineering, IIT (BHU), and Varanasi.

### References

1. Hench LL (1991) Bioceramics: From concept to clinic. *J Am Ceram Soc* 74: 1487-1510.
2. Clark AE, Hench LL (1976) The influence of surface chemistry on implant interface. *J Biomed Mater Res* 10: 161-174.
3. Hench LL (2006) The story of Bioglass. *J Mater Sci Mater Med* 17: 967-978.
4. Hench LL, Splinter RJ, Allen WC, Greenlee TK (1971) Bonding mechanisms at the interface of ceramic prosthetic materials. *J Biomed Mater Res Symp* 5: 117-141.
5. Kokubo T (1991) Bioactive glass ceramics: properties and applications. *Biomaterials* 12: 155-163.
6. LeGeros RZ (2002) Properties of osteoconductive biomaterials: calcium phosphates. *Clin Orthop Relat Res* 395: 81-98.
7. Cao W, Hench LL (1996) Bioactive Materials. *Ceramics International* 22: 493-507.
8. Rahaman MN, Day DE, Bal BS, Fu Q, Jung SB, et al. (2011) Bioactive glass in tissue engineering. *Acta Biomater* 7: 2355-2373.
9. Jung SB, Day DE, Day T, Stoecker W, Taylor P (2011) Treatment of non-healing diabetic venous stasis ulcers with bioactive glass nanofibers. *Wound Repair Regen*.
10. Neel EAA, Pickup DM, Valappil SP, Newport RJ, Knowles JC (2009) Bioactive functional materials: a perspective on phosphate-based glasses. *J Mater Chem* 19: 690-701.
11. Arstila H, Hupa L, Karlsson KH, Hupa M (2008) Influence of heat treatment on crystallization of bioactive glasses. *Journal of Non-Crystalline Solids* 354: 722-728.
12. Shirliff VJ, Hench LL (2003) Bioactive materials for tissue engineering, regeneration and repair. *Journal of Materials Science* 38: 4697-4707.
13. Li P, Zhang F, Kokubo T (1992) The effect of residual glassy phase in a bioactive glass-ceramic on the formation of its surface apatite layer in vitro. *Journal of Materials Science: Materials in Medicine* 3: 452-456.
14. Agathopoulos S, Tulaganov DU, Ventura JMG, Kannan S, Karakassides MA, et al. (2006) Formation of hydroxyapatite onto glasses of the CaO-MgO-SiO<sub>2</sub> system with B<sub>2</sub>O<sub>3</sub>, Na<sub>2</sub>O, CaF<sub>2</sub> and P<sub>2</sub>O<sub>5</sub> additives. *Biomaterials* 27: 1832-1840.
15. Marti A (2000) Inert bioceramics (Al<sub>2</sub>O<sub>3</sub>, ZrO<sub>2</sub>) for medical application. *Injury-international Journal of the Care of the Injured* 31: D33-D36.
16. Bharati S, Soundrapandian C, Basu D, Datta S (2009) Studies on a novel bioactive glass and composite coating with hydroxyapatite on titanium based alloys: Effect of  $\gamma$ -sterilization on coating. *J European Ceram Soc*, 29: 2527-2535.
17. Habibe AF, Maeda LD, Souza RC, Barboza MJR, Daguano JKM, et al. (2009) Effect of bioglass additions on the sintering of Y-TZP bioceramics. *Mater Sci Eng: C* 29: 1959-1964.
18. Singh D, de la Cinta Lorenzo-Martin M, Gutiérrez-Mora F, Routbort JL, Case ED (2006) Self-joining of zirconia/hydroxyapatite composites using plastic deformation process. *Acta Biomater* 2: 669-675.
19. Kokubo K, Ito S, Huang ZT, Hayashi T, Sakka S, et al. (1990) Solutions able to reproduce in vivo surface-structure changes in bioactive glass-ceramics A-W. *Journal of Biomedical Materials Research* 24: 721-734.
20. Greenspa DC, Hench LL (1976) Chemical and mechanical behavior of bioglass coated alumina. *J Biomed Materials Res* 10: 503-509.
21. Satoshi H, Kanji T, Chikara O, Akiyoshi O (1999) Mechanism of Apatite Formation on a Sodium Silicate Glass in a Simulated Body Fluid. *J Am Ceram Soc* 82: 2155-2160.
22. Toshihiro K, Yoshimasa H, Masayuki N, Mitsuo N (2001) Apatite Formation on Calcium Phosphate Invert Glasses in Simulated Body Fluid. *J Am Ceram Soc* 84: 450-452.
23. Clark AE, Pantano CG, Hench LL (1976) Auger spectroscopic analysis of Bioglass corrosion films. *J Am Ceram Soc* 59: 37-39.
24. Hanan HB, Khaled RM, El-Bassouini GT (2009) Fabrication and characterization of bioactive glass (45S5)/titania biocomposites. *Ceramics International* 35: 1991-1997.
25. Himanshu T, Sumit KH, Sampath KA, Uttam G, Singh SP, et al. (2015) Structural characterization and invitro bioactivity assessment of SiO<sub>2</sub>-CaO-P<sub>2</sub>O<sub>5</sub>-K<sub>2</sub>O-Al<sub>2</sub>O<sub>3</sub> glass as bioactive ceramic material. *Ceramics International* 41: 11756-11769.
26. ElBatal HA, Azooz MA, Khalil EMA, Soltan MA, Hamdy YM (2003) Characterization of some bioglass-ceramics. *Materials Chemistry and Physics* 80: 599-609.
27. Anthony LBM, Taek BK, Esther MV, Kathryn G, Richard KB, et al. (2015) A unified invitro evaluation for apatite-forming ability of bioactive glasses and their variants. *J Mater Sci: Mater Med* 26: 115.
28. Filgueiras MR, LaTorre GP, Hench LL (1993) Solution effects on the surface reactions of three bioactive glass compositions. *Journal of Biomedical Materials Research* 27: 1485-1493.
29. Filho OP, LaTorreGP, HenchLL (1996) Effect of crystallization on apatite layer formation of bioactive glass 45S5. *Journal of Biomedical Materials Research* 30: 509-514.
30. Stoch A, Jastrzebski W, Brozek A, Trybalska B, Cichocinska M, et al. (1999) FTIR monitoring of the growth of the carbonate containing apatite layers from simulated and natural body fluids. *Journal of Molecular Structure* 511-512: 287-294.
31. Balamurugan A, Balossier G, Kannan S, Michel J, Avit HS, et al. (2007) Development and in vitro characterization of sol-gel derived CaO - P<sub>2</sub>O<sub>5</sub> - SiO<sub>2</sub> - ZnO bioglass. *Acta Biomaterialia* 3: 255-262.
32. El-Batal FH, Khalil EM, Hamdy YM, Zidan HM, Aziz MS, et al. (2010) FTIR Spectral Analysis of Corrosion Mechanisms in Soda Lime Silica Glasses Doped with Transition Metal Oxides. *Silicon* 2: 41-47.
33. Elliot JC (1994) Structure and chemistry of the apatites and other calcium orthophosphates. Amsterdam: Elsevier Science.
34. Gisbon IR, Rehman I, Best SM, Bonfield W (2000) Characterization of the transformation from calcium-deficient apatite to b-tricalcium phosphate. *J Mater Sci* 12: 799-804.